 CMES, vol.48, no.3, pp.219-240, 2009

The Stress Analysis of Thin Contact Layers: a Viscoelastic Case

C. Y. Chen[1] **and C. Atkinson**[2]

Abstract: In this paper, we extend our previous analysis of a contact problem with a circular indenter pressed normally against a semi-infinite elastic composite to that of a semi-infinite viscoelastic composite which consists of a contact layer with uniform thickness welded together with another dissimilar medium. Using the correspondence principle between the Laplace transformed elastic equations and the viscoelastic ones, the asymptotic results derived previously for the pure elastic case are readily adopted for the viscoelastic one with the elastic constants replaced by appropriate functions of Laplace transformed variables for the linear viscoelastic solid. We focus our analysis on the force induced by the uniform indentation and investigate the effect of the contact layer and its property on the force generated. The Laplace transformed force is inverted using the method developed by Schapery to give the real time behaviour of the force.

Keywords: contact mechanics, viscoelastic composite, thin coating, force versus displacement

1 Introduction

Contact mechanics is a sub-branch of continuum mechanics that is concerned with the stresses and deformation of solid bodies in contact with each other. The stress field beneath an indenter and the associated deformation can be used to interpret and explain a variety of phenomena. Such contact may result in fracture which is intentional as in drilling, for example, or to be avoided in order to resist wear. Precise modelling for each of these events requires adequate constitutive equations describing the medium and the indenter as well as methods for solving the consequent boundary value problems.

Indentation tests or hardness tests are applications of contact mechanics that are commonly used in testing the mechanical properties of materials. For homoge-

[1] Department of Applied Mathematics, National University of Kaohsiung, Kaohsiung, Taiwan
[2] Department of Mathematics, Imperial College, Queen's Gate, London SW7 2BZ, U.K.

neous materials, the measured load or penetration response during elastic loading of an indentation test can be used to estimate the effective modulus. The identification of these effective moduli involving non-homogeneous materials, however, remains a challenging task in practice although various analytical efforts have been put forward in the study of load transfer between the contact bodies; see Selvadurai (2007) for a recent review.

For the indentation of a composite material such as a coated system (with a coating of thickness in the range of 0.2 microns to 5 microns) the effective modulus measured depends in an unknown way on the elastic properties of the coating and the semi-infinite substrate although substrate properties are more likely sensed when the coating is very thin than those sensed when the coating is much thicker. The nano-indentation technique has been established as the primary tool for investigating the hardness of small volumes of materials (Malzbender *et. al.* (2002); Cheng *et. al* (2004)). The atomic force microscope (AFM), for example, has been used as a microindenter of thin biological samples to determine the local elastic moduli of the tissue (Mahaffy *et. al* (2000); Dimitriadis *et.al.* (2002); Clifford and Seah (2009)). The microscope provides the signals for force and displacement and hence the force-indentation relation for the material, which can then be used to estimate elastic moduli, provided that a theoretical model describing the contact is available. Thus a simple-to-use model will be useful in the routine AMF work or other indentation tests in general.

Various numerical techniques such as the finite element method have been employed to optimize the nano-indentation experimental procedure and to support the evaluation of results ; see, for example, Liu and Tsai (2009); Chen (2002); Poon *et. al.* (2008); Henrich *et. al.* (2009) and the reference therein. Analytical solutions have also been put forward, for example, by Haider and Holmes (1997) providing an approximate solution for the indentation of a thin compressible elastic layer by a flat ended cylinder. This model is further extended and incorporated into a numerical scheme thereby improving the effectiveness of the scheme with the accuracy and convergence rate dramatically increased (Pavliotis and Holmes (2002)). By considering axisymmetric indentation of a thin incompressible elastic layer, Chadwick (2002) provided estimates for the force and contact radius by asymptotically matching a lubrication-type expansion in the contact region to the far field of an edge layer expansion. More recently, Chen and Atkinson (2008) proposed a semi-analytical formulation developed previously in solving fracture problems in layers to treat contact problems (Atkinson and Chen (1997); Chen and Atkinson (2005)). In particular, a singular perturbation technique is employed to obtain relatively explicit formulae for the situation when the layer is very thin and nano-indentation is used.

We continue the analysis carried out in Chen and Atkinson (2008) where a contact problem with a circular indenter pressed normally against a semi-infinite elastic composite is considered. The contact layer with uniform thickness (h) is welded together with another dissimilar medium of an infinite extent, as illustrated in Figure 1 . Using an integral equation formulation, the force exerted by the indenter on the contact layer is evaluated for finite h while an asymptotic formula in the limit $h \to 0$ is derived using singular perturbation techniques. A brief account of this is given in the appendix.

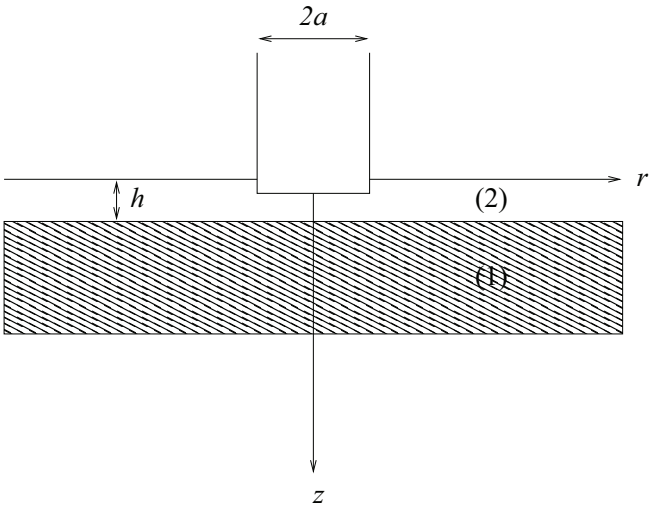

Figure 1: A circular indenter pressed normally against a layered composite.

Here we extend the results for the pure elastic composite further to consider the viscoelastic case. It is well known that a correspondence principle exists between the Laplace transformed viscoelastic equations and the elastic ones. It is therefore relatively simple to go from the solution for an elastic problem to a viscoelastic one. To avoid repetition, we will omit the detailed formulation of the elastic model, the reader is referred to Chen and Atkinson (2008) for details, and list some of the basic equations for the theory of viscoelasticity for small strain. The constitutive equations relating the stress to the history of strain can be written, for an isotropic solid, as

$$s_{ij} = \int_{-\infty}^{t} G(t-\tau)\frac{\mathrm{d}e_{ij}}{\mathrm{d}\tau}\mathrm{d}\tau,$$

and

$$\sigma_{kk} = \int_{-\infty}^{t} H(t-\tau)\frac{\mathrm{d}\varepsilon_{kk}}{\mathrm{d}\tau}\mathrm{d}\tau,$$

where the deviatoric components are defined as

$$s_{ij} = \sigma_{ij} - \frac{1}{3}\delta_{ij}\sigma_{kk}, \quad \text{and} \quad e_{ij} = \varepsilon_{ij} - \frac{1}{3}\delta_{ij}\varepsilon_{kk},$$

and the repeated suffices sum over 1, 2, and 3. As usual, $\varepsilon_{ij} = \frac{1}{2}\left(\frac{\partial u_i}{\partial x_j} + \frac{\partial u_j}{\partial x_i}\right)$ is the definition of small strain (see Christensen (1971)). An alternative representation to the integral notation in the form of differential operators is given as

$$P s_{ij} = Q e_{ij} \quad \text{and} \quad M\sigma_{kk} = N\varepsilon_{kk},$$

where P, Q, M and N are polynomials in the time derivative $\partial/\partial t$. The equations of motion which are the same for both the pure elastic and viscoelastic cases are

$$\rho\frac{\partial^2 u_i}{\partial t^2} = \sigma_{ij,j},$$

where ρ is the density of the material.

As can be easily seen, the existence of the correspondence principle ensures that the Laplace transforms of the above equations of motion and the constitutive equation are identical to those of the elasticity equations with the elastic moduli replaced by appropriate functions of p, the Laplace transform variable. Thus

$$\bar{s}_{ij}(p) = p\bar{G}(p)\,\bar{e}_{ij}(p) \quad \text{and} \quad \bar{\sigma}_{kk}(p) = p\bar{H}(p)\,\bar{\varepsilon}_{kk}(p), \tag{1.1}$$

where

$$\bar{G}(p) = \int_0^{\infty} e^{-pt}\,G(t)\mathrm{d}t \quad \text{and} \quad \bar{H}(p) = \int_0^{\infty} e^{-pt}\,H(t)\mathrm{d}t,$$

and $p\bar{G}_i(p)$ corresponds to an elastic constant. The equations of motion for the plane strain case, ignoring the inertia terms, become

$$\frac{\partial\bar{\sigma}_{ij}}{\partial x_j} = 0, \quad i,j = 1,2, \tag{1.2}$$

where in all the above equations it is assumed that all variables are zero prior to time $t = 0$.

As a first example, the standard linear solid is considered and using the differential operator notation, the constitutive equations are

$$\left(\frac{\mathrm{d}}{\mathrm{d}t}+\beta\right)s_{ij} = a_0\left(\frac{\mathrm{d}}{\mathrm{d}t}+\alpha\right)e_{ij}, \tag{1.3}$$

$$\left(\frac{\mathrm{d}}{\mathrm{d}t}+\eta\right)\sigma_{kk} = b_0\left(\frac{\mathrm{d}}{\mathrm{d}t}+\zeta\right)\varepsilon_{kk}, \tag{1.4}$$

where $\alpha,\beta,\eta,\zeta,a_0$, and b_0 are positive constants. Taking the Laplace transform of the above equations and using equation (1.1), we have

$$p\bar{G}(p)=a_0\left(\frac{p+\alpha}{p+\beta}\right), \quad \text{and} \quad p\bar{H}(p)=b_0\left(\frac{p+\zeta}{p+\eta}\right). \tag{1.5}$$

We shall adopt a common approximation for viscoelastic solids by taking Poisson's ratio ν to be constant. It can be deduced that

$$\bar{H}(p)=\left(\frac{\nu+1}{1-2\nu}\right)\bar{G}(p),$$

and the time transformed elastic constants become

$$2\bar{\mu}(p)=p\bar{G}(p), \quad \bar{\lambda}(p)=\frac{1}{3}\left(p\bar{H}(p)-p\bar{G}(p)\right) \quad \text{and} \quad \bar{E}(p)=\left(\frac{\nu+1}{3}\right)p\bar{G}(p). \tag{1.6}$$

The relaxation functions can be inverted to give

$$G(t) = a_0\left\{\left(\frac{\alpha}{\beta}\right)-\left(\frac{\alpha-\beta}{\beta}\right)e^{-\beta t}\right\}, \tag{1.7}$$

$$H(t) = a_0\left(\frac{\nu+1}{1-2\nu}\right)\left\{\left(\frac{\alpha}{\beta}\right)-\left(\frac{\alpha-\beta}{\beta}\right)e^{-\beta t}\right\}. \tag{1.8}$$

2 Force versus displacement - the pure elastic case

An asymptotic formula for the total force F in the limit $h\to 0$ has been derived for the pure elastic case in Chen and Atkinson (2008). Some typos unfortunately have appeared in the previous work (Section 5 -Force versus displacement). We correct these typos here and repeat part of the analysis for the force induced by a uniform indentation when h is infinitesimal before extending it to the viscoelastic case.

To evaluate the total force F exerted by the punch on the elastic composite we require

$$F = -2\pi\int_0^a r\left(\sigma_{33}^{(2)}\right)_{z=0}\mathrm{d}r, \tag{2.1}$$

where a is the radius of the circular indenter and $\sigma_{33}^{(2)}$ is the normal stress acting on the surface of the contact layer $z = 0$. With the formulation,

$$r\left(\sigma_{33}^{(2)}\right)_{z=0} = \frac{\partial}{\partial r}\left(\int_r^a \frac{ug(u)\mathrm{d}u}{\sqrt{t^2-r^2}}\right), \tag{2.2}$$

thus

$$\frac{F}{2\pi} = \int_0^a g(u)\,\mathrm{d}u. \tag{2.3}$$

The density function $g(u)$ satisfies the equation

$$g(u) = \frac{2}{\pi}\left(\frac{\mu_2}{1-\nu_2}\right)\delta_0 + \frac{2}{\pi}\left(\frac{\mu_2}{1-\nu_2}\right)\int_0^a g(t)\,I(u,t)\mathrm{d}t, \tag{2.4}$$

for $0 < u < a$, where μ_2 and ν_2 are elastic constants for the contact layer (medium 2) and

$$I(u,t) = \int_0^\infty \mathscr{F}(\rho,h)\cos(u\rho)\cos(t\rho)\mathrm{d}\rho, \tag{2.5}$$

with

$$\mathscr{F}(\rho,h) = \left(\frac{1-\nu_2}{\mu_2}\right)\left[1-\left(\frac{\gamma_5-\gamma_3\rho h e^{-2\rho h}-\gamma_4 e^{-4\rho h}}{\gamma_5+\gamma_3\rho^2h^2e^{-2\rho h}+\gamma_1 e^{-2\rho h}+\gamma_4 e^{-4\rho h}}\right)\right], \tag{2.6}$$

h being the thickness of the contact layer and γ's being functions of elastic constants. See appendix for the derivation of the density function $g(u)$.

We can express (2.3) as

$$\frac{F}{2\pi} = \int_0^{a-\varepsilon} g(u)\,\mathrm{d}u + \int_{a-\varepsilon}^a g(u)\,\mathrm{d}u, \tag{2.7}$$

where ε is such that $h << \varepsilon << a$. This means that $\varepsilon \to 0$ and $h/\varepsilon \to 0$ as $h \to 0$ but ε is otherwise arbitrary; one could choose $\varepsilon = h^{1/3}$ for example (compare Atkinson and Leppington (1983) for other examples where this idea is used).

When $h/a << 1$, to leading order, the indenter hardly notices the layer except near its end at $u = a$. Thus, to analyse the behaviour and derive a solution for $g(u)$ near $u = a$ in the limit $h \to 0$, an inner coordinate X is defined which relates to the outer coordinate u by $u = a + hX$ for $-a/h < X < 0$ with $G_-(X) = g(a+hX)$. An analytical method is developed for these coordinates and summarised in the appendix. The outer approximation for $g(u)$, denoted by $g^{(o)}(u)$, will thus be used in the first integral of equation (2.7) and the inner approximation, $G_-(X)$, in the

second. Again, the inner and outer approximations used below in (2.8) and (2.12) are derived in Chen and Atkinson (2008), we therefore refer the reader to the afore mentioned paper for details.

Using the outer approximation $g^{(o)}(u)$ below

$$\begin{aligned} g^{(o)}(u) \;=\; & \frac{2\,\delta_0}{\pi}\left(\frac{\mu_1}{1-\nu_1}\right) \\ & + h\left\{\beta_0\left(\frac{1}{a-u}+\frac{1}{a+u}\right)+\alpha_0\left[1+C_1\left(\frac{\mu_2}{1-\nu_2}\right)\right]\delta(a-u)\right\} \\ & + h^2\left\{\gamma_0\left[\log(a-u)+\log(a+u)\right]-\frac{\alpha_0 C_2}{\pi}\left(\frac{\mu_2}{1-\nu_2}\right)\left(\frac{1}{(a-u)^2}+\frac{1}{(a+u)^2}\right)\right\}, \end{aligned} \tag{2.8}$$

and integrating, we have

$$\begin{aligned} \int_0^{a-\varepsilon} g^{(o)}(u)\,\mathrm{d}u \;=\; & \frac{2\delta_0}{\pi}\left(\frac{\mu_1}{1-\nu_1}\right)(a-\varepsilon)+h\,\beta_0[-\log\varepsilon+\log(2a-\varepsilon)] \\ & + h^2\left[\frac{g(a)}{4a^2}\left(\frac{C_2}{\pi}\right)^2\left(\frac{\mu_1}{1-\nu_1}\right)^2(2a\log(2a-\varepsilon)-2(a-\varepsilon)-\varepsilon\log(\varepsilon(2a-\varepsilon))) \right. \\ & \left. -\alpha_0\frac{C_2}{\pi}\left(\frac{\mu_2}{1-\nu_2}\right)\left(\frac{1}{\varepsilon}-\frac{1}{2a-\varepsilon}\right)\right], \end{aligned} \tag{2.9}$$

where δ_0 is the depth of indentation and μ_1 and ν_1 are elastic constants for the substrate layer (medium 1). The constants α_0, β_0 and γ_0 are determined through matching and

$$C_1 = \frac{1-\nu_2}{\mu_2}-\frac{1-\nu_1}{\mu_1}, \quad C_2 = -\left(\frac{1-\nu_1}{\mu_1}\right)m_1,$$

with m_1 given by (A.17) in the appendix.
Since $\varepsilon << a$, we can expand $\log(2a-\varepsilon)$ to obtain

$$\begin{aligned} & \int_0^{a-\varepsilon} g^{(o)}(u)\,\mathrm{d}u \;= \\ & \qquad \frac{2\delta_0}{\pi}\left(\frac{\mu_1}{1-\nu_1}\right)(a-\varepsilon)+h\,\beta_0\left(\log 2a-\log\varepsilon-\frac{\varepsilon}{2a}+O((\varepsilon/2a)^2)\right)+O(h^2). \end{aligned} \tag{2.10}$$

To evaluate $\int_{a-\varepsilon}^{a} g(u)\,\mathrm{d}u$, we rewrite this in inner coordinates so

$$\int_{a-\varepsilon}^{a} g(u)\,\mathrm{d}u \;=\; h\int_{-\varepsilon/h}^{0} G_{-}(X)\,\mathrm{d}X, \tag{2.11}$$

and the expansion as $X \to -\infty$, using the inner approximation, is conveniently written as

$$G_{-}(X) \;=\; B\left(1-\frac{m_0}{\pi}\delta(-X)-\frac{m_1}{\pi}\frac{1}{(X-1)}-\frac{m_2}{(X-1)^2}\right)+G_1(X), \tag{2.12}$$

for $X<0$; B and β_0 are given by

$$B \;=\; \hat{B}+h\frac{\beta_0}{2a}, \quad \hat{B} \;=\; \frac{2\delta_0}{\pi}\left(\frac{\mu_1}{1-\nu_1}\right), \quad \text{and} \quad \beta_0 \;=\; \frac{m_1}{\pi}\hat{B}, \tag{2.13}$$

and $\delta(-X)$ is non-zero at 0^{-} to be consistent with previous asymptotic results. The constants m_0, m_1 and m_2 are functions of elastic constants (see equations (A.16) and (A.17) in appendix), the detailed formulations are omitted here. Note that the capital $G_{-}(X)$ or $G_1(X)$ notation is used here to denote the inner coordinate of the function $g(u)$, it is not to be confused with the relaxation functions $G_1(t)$ and $G_2(t)$ in the previous sections.

It follows that

$$\begin{aligned}\int_{a-\varepsilon}^{a} g(u)\,\mathrm{d}u \sim hB\left[\frac{\varepsilon}{h}-\frac{m_0}{\pi}+\frac{m_1}{\pi}\log\left(\frac{\varepsilon}{h}+1\right)+m_2\left(-1+\frac{1}{\varepsilon/h+1}\right)\right]\\ +h\int_{-\infty}^{0} G_1(X)\,\mathrm{d}X, \quad \text{as} \quad \varepsilon/h\to\infty.\end{aligned} \tag{2.14}$$

Writing

$$\overline{G}_{1-}(\xi) \;=\; \int_{-\infty}^{0} G_1(X)\,e^{i\xi X}\,\mathrm{d}X, \tag{2.15}$$

then

$$\overline{G}_{1-}(\xi) \;=\; \overline{G}_{-}(\xi)-\frac{B}{i\xi}+\frac{Bm_0}{\pi}+\frac{Bm_1}{\pi}\int_{-\infty}^{0}\frac{e^{i\xi X}\,\mathrm{d}X}{(X-1)}+Bm_2\int_{-\infty}^{0}\frac{e^{i\xi X}\,\mathrm{d}X}{(X-1)^2}. \tag{2.16}$$

Taking the limit of $\overline{G}_{1-}(\xi)$ as $\xi\to 0$ with

$$\overline{G}_{-}(\xi) \;=\; B\left(\frac{1}{i\xi}-\frac{m_0}{\pi}-\frac{m_1}{\pi}\log(i\xi)+m_2\,(i\xi)\log(i\xi)+\cdots\right), \tag{2.17}$$

and using the asymptotic results

$$\int_{-\infty}^{0} \frac{e^{i\xi X}\,\mathrm{d}X}{(X-1)} \;=\; \left(\gamma+\log\xi+\frac{i\pi}{2}\right)+i\xi\left(\gamma+\log\xi+\frac{i\pi}{2}\right)+O(\xi^2),$$

with $\gamma = 0.577215665$ being Euler constant and

$$\int_{-\infty}^{0} \frac{e^{i\xi X}\,\mathrm{d}X}{(X-1)^2} \;=\; 1+i\xi\left(\gamma+\log\xi+\frac{i\pi}{2}\right)+O(\xi^2),$$

gives

$$\lim_{\xi\to 0}\overline{G}_{1-}(\xi) \;=\; \frac{Bm_1}{\pi}\gamma+Bm_2+O(\xi). \tag{2.18}$$

Thus substituting into equation (2.14) and using (2.13), we get

$$\int_{a-\varepsilon}^{a} g(u)\,\mathrm{d}u \;=\; \hat{B}\varepsilon \;+\; h\left[\frac{\beta_0\varepsilon}{2a} \;+\; \hat{B}\left(-\frac{m_0}{\pi}+\frac{m_1\gamma}{\pi}+\frac{m_1}{\pi}\log\left(\frac{\varepsilon}{h}\right)\right]\right)+O(h^2). \tag{2.19}$$

Summing equations (2.10) and (2.19) gives, correct to order h, with $\hat{B}$ and β_0 given by (2.13),

$$\frac{F}{2\pi}=\frac{2\delta_0}{\pi}\left(\frac{\mu_1}{1-\nu_1}\right)\left[a+h\left(\frac{m_1}{\pi}(\log 2a+\gamma-\log h) \;-\; \frac{m_0}{\pi}\right)\right]+O(h^2). \tag{2.20}$$

Significantly, the result of equation (2.20) is independent of ε assuming only that $\varepsilon/h\to\infty$.

The asymptotic result is verified below: in Figure 2(a) the total force F is plotted for $\mu_1/\mu_2 = 2$ where the dotted line nearer to $h = 0$ is the asymptotic result given by equation (2.20) and the solid line for finite h is given by (2.3) and (2.4). The curves show good agreement where the dotted-line overlaps with the solid line. In Figure 2 (b), the total force is plotted for fixed values of h while μ_1/μ_2 is allowed to vary. As expected, all curves intersect at the point when $\mu_1/\mu_2 = 1$ and, while holding μ_2 fixed, the smaller h is, the larger the effect of increasing μ_1/μ_2 has on the total force. The force F shown in Figure 2 has been normalised by F_e which is induced by a uniform indentation in medium 2 alone, i.e. $F_e = \lim_{h\to\infty} F$.

To give a measure of the effect of the layer and its property on the force generated by the uniform indentation, we differentiate the force of equation (2.20) with respect to the layer thickness h and show the result in Figure 3 as the property of

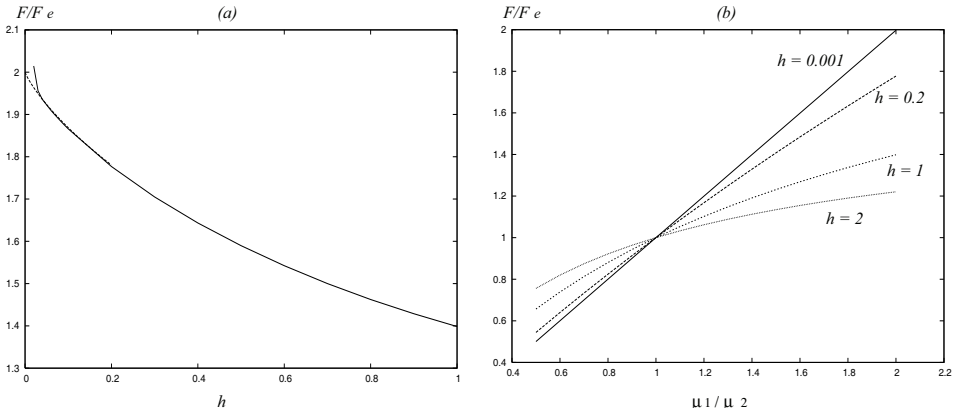

Figure 2: (a) The asymptotic and numerical results for F with $\mu_1/\mu_2 = 2$; (b) the resulting force F for varying μ_1/μ_2 (μ_2 fixed) with different fixed values of h.

medium 2 (μ_2) varies while holding the substrate (medium 1) fixed. The result suggests that as $h \to 0$, the force generated becomes more sensitive to changes in the contact layer, i.e. dF/dh increases as μ_2 increases and this effect becomes more pronounced as $h \to 0$. The result here can also be used to help identify the property of a material, for example, in an experiment where a nano-indenter is used to press into a material of unknown property (medium 2) which can be a very fine powder or layer resting on some substrate (medium 1) of known property. From equation (2.20), we have as $h \to 0$,

$$\frac{dF}{dh}\left(\frac{1-\nu_1}{\mu_1}\right)\frac{\pi}{2\delta_0} = \frac{m_1}{\pi}(\log 2a + \gamma - 1) - \frac{m_0}{\pi} - \frac{m_1}{\pi}\log h + O(h).$$

If we write $Y_1 = -\dfrac{1}{\log h}$, this gives

$$Y_1\frac{dF}{dh}\left(\frac{1-\nu_1}{\mu_1}\right)\frac{\pi}{2\delta_0} = \frac{m_1}{\pi} + Y_1\left(\frac{m_1}{\pi}(\log 2a + \gamma - 1) - \frac{m_0}{\pi}\right) + O(Y_1 h).$$

Hence plotting the left hand side versus Y_1 from experiments as $h \to 0$ would give a straight line intersecting the axis $Y_1 = 0$ at m_1/π and with slope

$$\frac{m_1}{\pi}(\log 2a + \gamma - 1) - \frac{m_0}{\pi}.$$

With the properties of the substrate, i.e. ν_1 and μ_1 known, we thus have two equations to determine ν_2 and μ_2. The expressions of m_0 and m_1 are given by (A.16) and (A.17) in the appendix.

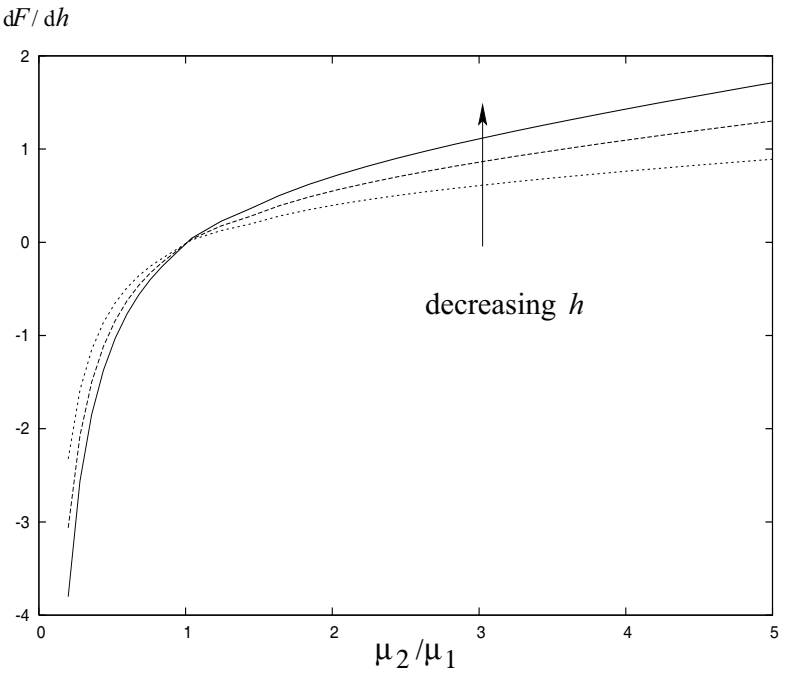

Figure 3: The numerical results for dF/dh with varying μ_2/μ_1 while holding μ_1 fixed for $h = 10^{-3}, 10^{-4}, 10^{-5}$.

3 Time-dependent force - viscoelastic case

Using the correspondence principle and the asymptotic formula for the total force exerted on the contact layer when h is small (equation (2.20)), the Laplace transformed time-dependent force can be written as, for $h \to 0$,

$$\frac{\bar{F}(p)}{2\pi} = \frac{2}{\pi}\left(\frac{\bar{\mu}_1(p)}{1-\nu_1}\right)\frac{\delta_0}{p}\left[a + h\left(\frac{\bar{m}_1}{\pi}(\log 2a + \gamma - \log h) - \frac{\bar{m}_0}{\pi}\right)\right] + O(h^2), \quad (3.1)$$

where $\bar{m}_1$ and $\bar{m}_0$ are functions of elastic constants which are now replaced by appropriate functions of p.

To obtain the real time behaviour of the force, we invert $\bar{F}(p)$ numerically using the method developed by Schapery. The method assumes that the function $F(t)$ is of the form

$$F(t) = F_\infty + \sum_{i=1}^{n} A_i e^{-x_i t}, \quad (3.2)$$

where F_∞ is the residue given by the pole at the origin $p=0$ and x_i's are prescribed positive constants. The unknown coefficients A_i's are to be determined from the set of simultaneous equations

$$\left[\bar{F}(p)-\frac{F_\infty}{p}\right]_{p\to x_i} = \left[\sum_{j=1}^{n}\frac{A_j}{p+x_j}\right]_{p\to x_i}. \tag{3.3}$$

With an explicit formula (3.1) available for small h, the time-dependent force can be calculated with relative ease. The asymptotic formula, however, is no longer valid when h becomes large. In this case, we derive the time dependent force $F(t)$ by first evaluating the time-dependent density function $g(u,t)$ which for the pure elastic case is given by (2.4), namely,

$$g(u) = \frac{2}{\pi}\left(\frac{\mu_2}{1-\nu_2}\right)\delta_0 + \frac{2}{\pi}\left(\frac{\mu_2}{1-\nu_2}\right)\int_0^a g(r)\,I(u,r)\,\mathrm{d}r, \tag{3.4}$$

and

$$I(u,r) = \int_0^\infty \mathscr{F}(\rho,h)\cos(u\rho)\cos(r\rho)\mathrm{d}\rho, \tag{3.5}$$

where $0<u<a$ and $\mathscr{F}(\rho,h)$ is given by (2.6). Using the correspondence principle, the Laplace transformed $\bar{g}(u,p)$ becomes

$$\bar{g}(u,p) = \frac{2}{\pi}\left(\frac{\bar{\mu}_2}{1-\nu_2}\right)\frac{\delta_0}{p} + \frac{2}{\pi}\left(\frac{\bar{\mu}_2}{1-\nu_2}\right)\int_0^a \bar{g}(r,p)\,\bar{I}(u,r,p)\,\mathrm{d}r, \tag{3.6}$$

and

$$\bar{I}(u,r,p) = \int_0^\infty \bar{\mathscr{F}}(\rho,h,p)\cos(u\rho)\cos(r\rho)\mathrm{d}\rho, \tag{3.7}$$

with the elastic constants in $\bar{\mathscr{F}}(\rho,h,p)$ replaced by appropriate functions of p. To invert the integral for the real time $g(u,t)$, again we assume the time-dependent density function is of the form

$$g(u,t) = g_\infty(u)+\sum_{i=1}^{n}A_i(u)\,e^{-x_i t}, \quad 0<u<a, \tag{3.8}$$

where $g_\infty(u)$ is the residue given by the pole at the origin $p=0$, then

$$\left[\bar{g}(u,p)-\frac{g_\infty(u)}{p}\right]_{p\to x_i} = \left[\sum_{j=1}^{n}\frac{A_j(u)}{p+x_j}\right]_{p\to x_i}. \tag{3.9}$$

To find $g_\infty(u)$, we write

$$\bar{g}(u,p) \;=\; \frac{g_\infty(u)}{p} + \hat{g}(u,p), \tag{3.10}$$

and $\hat{g}(u,p)$ is analytic at $p=0$. Substituting back into the integral equation, multiplying throughout by p and taking the limit $p \to 0$ give,

$$g_\infty(u) \;=\; \frac{2}{\pi}\left(\frac{\mu_{2\infty}}{1-\nu_2}\right)\delta_0 \;+\; \frac{2}{\pi}\left(\frac{\mu_{2\infty}}{1-\nu_2}\right)\int_0^a g_\infty(r)\,\bar{I}_\infty(u,r)\,\mathrm{d}r, \tag{3.11}$$

where

$$I_\infty(u,r) \;=\; \lim_{p\to 0}\bar{I}(u,r,p) \quad \text{and} \quad \mu_{2\infty} = \lim_{p\to 0}\bar{\mu}_2(p). \tag{3.12}$$

The function $g_\infty(u)$ can now be evaluated numerically by dividing the range of integration from 0 to a into n intervals. This then gives us a system of $n+1$ equations and $n+1$ unknowns. These unknown $g_\infty(u_i)$'s, $i = 1,2,\cdots n+1$, are found by inverting a $(n+1)\times(n+1)$ matrix. Equation (3.6) is similarly discretised to evaluate $\bar{g}(u_i,p)$'s for each $p = x_i$ and subsequently, the formula (3.9) is applied to find $A_j(u_i)$ at each u_i for $i = 1,2,\cdots,n+1$. The real time $g(u,t)$ can now be computed using (3.8) which is further integrated to give the total force $F(t)$ for finite h.

4 Numerical simulations

To illustrate the viscoelastic effect on the force induced by a fixed displacement, three cases are considered below in which the contact layer, medium 2, is viscoelastic while medium 1 is elastic. In each case, the corresponding relaxation functions are plotted to show the relative stiffness of the media and the time-dependent forces are given with different values of layer thickness h to illustrate the effect of the contact layer. The resulting force is normalised by that of an indentation in a single medium (medium 1) for comparison. The relaxation functions $G_1(t)$ and $G_2(t)$ are computed using equation (1.7) with the subscript indicating the appropriate medium. The fixed parameter values taken for all three cases are

$$\alpha_1 = \beta_1, \quad \alpha_2 = 0.5, \quad \beta_2 = 0.8, \quad a_{01} = 2.4, \tag{4.13}$$

while a_{02} varies for each case; a_{01} and a_{02} represent the constant a_0 of equation (1.7) for medium 1 and medium 2 respectively. Additionally, Poisson's ratios, $\nu_1 = \nu_2 = 0.3$, are taken to be constant throughout for both media and the indentation depth $\delta_0 = 0.1$ is fixed for all three cases.

The results show that the force relaxes as the material (medium 2) relaxes; in Figure 4, as the property of medium 2 approaches that of medium 1, the normalised force

tends to unity and as the contact layer becomes smaller (h decreases), the closer it is to unity. In Figure 5, $G_1(0) < G_2(0)$ and $G_1(\infty) > G_2(\infty)$, we thus expect $F(0) > 1$ and $F(\infty) < 1$; while in Figure 6, $G_1(t) > G_2(t)$ and thus $F(t) < 1$ for all time and $F(t)$ decreases as the material relaxes with time.

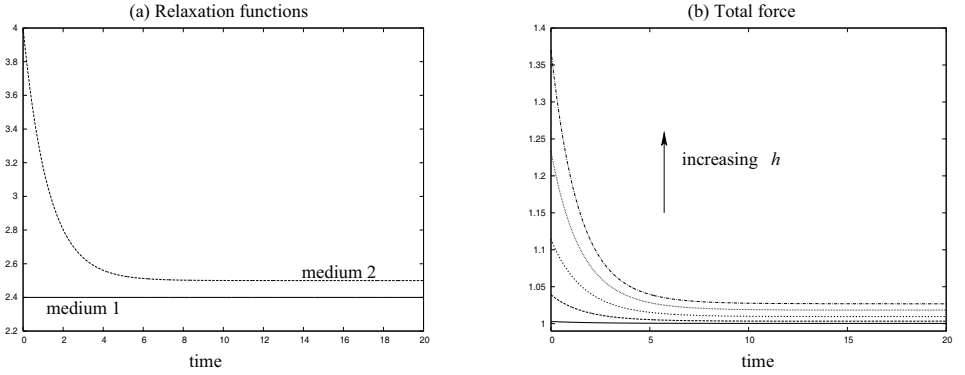

Figure 4: (a) Relaxation functions and (b) the corresponding time-dependent forces with the layer thickness $h = 2, 1, 0.4, 0.1, 0.01$ and $a_{02} = 4$.

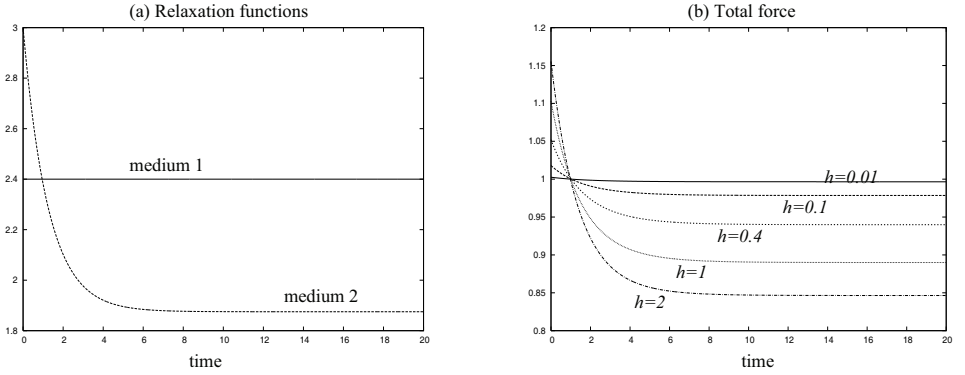

Figure 5: (a) Relaxation functions and (b) the corresponding time-dependent forces; $a_{02} = 3$.

The time dependent effect of the layer on the force induced as the material relaxes is shown in Figure 7 in which medium 1 is assumed elastic and medium 2 viscoelastic. As medium 2 relaxes with time, the force becomes less sensitive to the changes in medium 2 and so dF/dh decreases as t increases and this sensitivity reduces as h becomes large. This result is consistent with that shown in Figure 3 for the pure elastic case where dF/dh increases as μ_2 increases and h decreases.

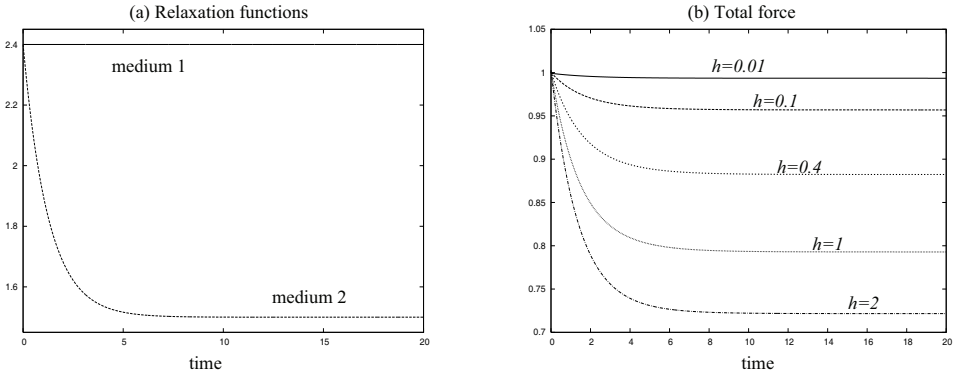

Figure 6: (a) Relaxation functions and (b) the corresponding time-dependent forces; $a_{02} = 2.4$.

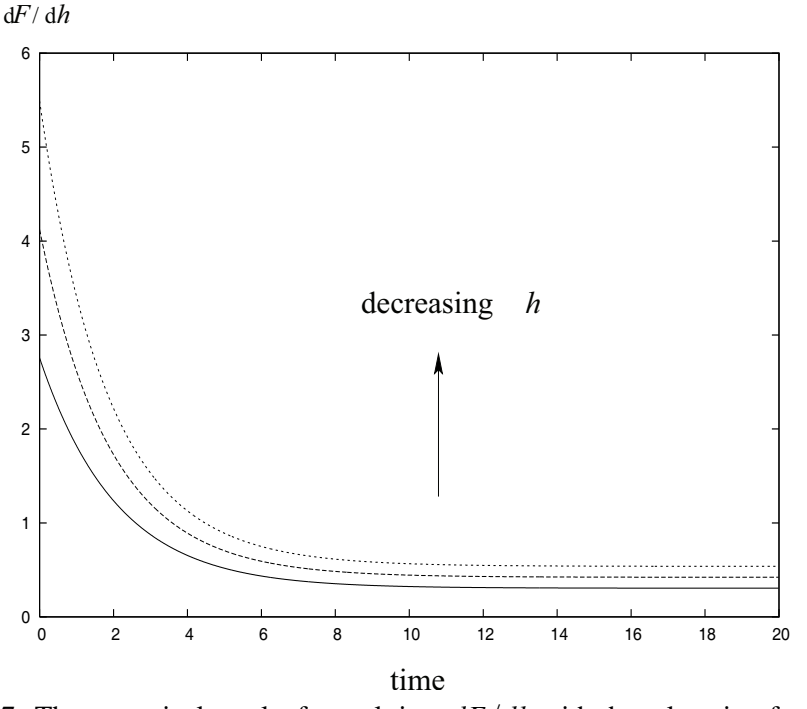

Figure 7: The numerical results for real time dF/dh with the relaxation functions given by Figure 4 (a); $h = 10^{-3}, 10^{-4}$ and 10^{-5}.

5 Conclusion

This paper extends a previous paper by Chen and Atkinson (2008) to deduce force - displacement curves, in particular, for thin coating on known substrates enabling the determination of properties of the coating material. Methods are developed which apply to the contact problem and give analytic results. Earlier work developing these singular perturbation methods for fracture problems is described in Atkinson and Chen (1997) and Chen and Atkinson(2005). The methods developed here should apply to cases when the layer is infinitesimal.

Nano-indentation techniques have been established as the primary tool for investigating the hardness of small volumes of materials (Malzbender *et. al.* 2002; Cheng and Cheng 2004). The atomic force microscope (AFM) has been used as a micro-indenter of thin biological samples to determine the local elastic moduli of the tissue (Mahaffy *et. al.* 2000; Dimitriadis , *et. al.* 2002). The microscope provides the signals for force and displacement, and hence the force-indentation relationship for the material, which can then be used to estimate the elastic moduli, provided that a theoretical model describing the contact is available. Thus, a simple-to-use model will be useful in the routine AMF work and indentation tests in general. A model that provides an approximate solution for the indentation of a thin compressible elastic layer by a flat-ended cylinder has been developed by Haider and Holmes (1997). By considering the axisymmetric indentation of a thin incompressible elatic layer, Chadwick (2002) provided estimates for the force and contact radius by asymptotically matching a lubrication-type expansion in the contact region to the far field of an edge layer expansion.

In priciple, the limit result of Section 2 when $h \to 0$, i.e.

$$Y_1 \frac{dF}{dh}\left(\frac{1-\nu_1}{\mu_1}\right)\frac{\pi}{2\delta_0} = \frac{m_1}{\pi} + Y_1\frac{m_1}{\pi}(\log 2a + \gamma - 1) - \frac{m_0}{\pi} + O(Y_1 h),$$

can be extended to other contact shapes. This result allows one to deduce layer properties in both the elastic and viscoelastic cases, although some numerical inversion of the Laplace transform is of course required in the viscoelastic case.

Acknowledgement: The first author would like to thank the National Science Council of Taiwan for their financial support.

References

Atkinson, C.; Chen, C.Y. (1997): The influence of layer thickness on the stress intensity factor of a crack lying in an (visco)elastic layer embedded in a different (visco)elastic medium. (Mode I analysis). *Proc. R. Soc. Lond.*, A**453**, 1445-1471.

Atkinson, C.; Leppington, F.G. (1983): The asymptotic solution of some integral equations. *IMA J. Appl. Math.* **31**, 169-182.

Chadwick, R.S. (2002): Axisymmetric indentation of a thin incompressible elastic layer. *SIAM J. Appl. Math.* **62**, 1520-1530.

Chen, C.Y.; Atkinson C. (2005): The influence of layer thickness on the stress intensity factor of a penny-shaped crack lying in a sandwiched viscoelastic bimaterial. *Int. J. Eng. Sci.*, **43**, 222-249.

Cheng, Y.T.; Cheng C.M. (2004): Scaling, dimensional analysis, and indentation measurements. *Mater. Sci. Eng. R.*, **44**, 91.

Chen, C.Y.; Atkinson, C. (2008): The stress analysis of thin contact layers: a singular perturbation method for integral equations. *Proc. R. Soc. Lond.* A**464**, 1439-1459.

Chen, J. (2002): Computational Simulations of micro-indentation tests using gradient plasticity. *CMES: Computer Modeling in Engineering & Sciences* **3(6)**, 743-754.

Christensen R.M. (1971): *An introduction to the theory of viscoelasticity*, Academic Press, London.

Clifford C.A.; Seah M.P. (2009): Nanoindentation measurement of Young's modulus for compliant layers on stiffer substrates including the effect of Poisson's ratios. *Nanotech.* **20(14)**, article no. 145708.

Dimitriadis, E.K.; Horkay, F.; Maresca, J.; Kachar, B.; Chadwick, R. S. (2002): Determination of elastic moduli of thin layers of soft material using the atomic force microscope. *Biophys. J.* **82**, 2798-2810.

Green, A.E.; Zerna W. (1968): *Theoretical elasticity*, Oxford University Press, London. **Haider, M.A.; Holmes, M.H.** (1997) A mathematical approximation for the soltion for a static indentation test. *J. Biomech.* **3**, 747-751.

Heinrich, C.; Waas, A.M.; Wineman, A.S. (2009): Determination of material properties using nanoindentation and multiple indenter tips. *Int. J. Solids Struct.* **46(2)**, 364-376.

Liu, D.S.; Tsai, C.Y. (2009): Estimation of thermo-elasto-plastic properties of thin-film mechanical properties using MD nanoindentation simulations and an inverse FEM/ANN computational scheme. *CMES: Computer Modeling in Engineering & Sciences* **39(1)**, 29-47.

Mahaffy, R.E.; Shih, C.K.; Mackintosh, F.C.; Kas, J. (2000): Scanning probe-based frequency dependent microrheology of polymer gels and biological cells. *Phys. Rev. Lett.* **85**, 880-883.

Malzbender, J.; den Toonder, J. M. J.; Balkenende, A. R.; de With, G. (2002):

A methodology to determine the mechanical properties of thin films with application to nano-particle filled methyltrimethoxysilane sol-gel coatings. *Mater. Sci. Eng. R.* **36** 47.

Pavliotis G.A.; Holmes M.H. (2002): A perturbation-based numerical method for solving a three-dimensional axisymmetric indentation problem *J. Eng. Math.* **43(1)**, 1-17.

Poon, B.; Rittel, D.; Ravichandran, G. (2008): An analysis of nanoindentation in elasto-plastic solids. *Int. J. Solids Struct.* **45(25-26)**, 6399-6415.

Selvadurai, A.P.S. (2007): The analytical method in geomechanics. *Appl. Mech. Rev.* **60**, 87-106.

Van Dyke, M. (1975): *Perturbation methods in fluid mechanics*, The Parabolic Press, California.

Appendix

A brief description of the analysis which was carried out for the contact problem in a pure elastic composite is given below, the reader is referred to Chen and Atkinson (2008) for details. There were typos in the previous work which have been corrected below. By taking the double Fourier Transform of the equation of motion (1.2) for the pure elastic case, a relationship between the transformed stress and displacement on the contact boundary $z=0$ is obtained, namely,

$$\bar{\bar{\sigma}} = \kappa(\rho,h)\bar{\bar{u}}, \quad \kappa(\rho,h) = \rho\left(\frac{\mu_2}{1-\nu_2}\right)\left(\frac{\gamma_5+\gamma_3\rho^2h^2e^{-2\rho h}+\gamma_1e^{-2\rho h}+\gamma_4e^{-4\rho h}}{\gamma_5-\gamma_3\rho he^{-2\rho h}-\gamma_4e^{-4\rho h}}\right), \tag{A.1}$$

with $\bar{\bar{\sigma}}$ and $\bar{\bar{u}}$ denoting the transformed normal stress $\sigma_{33}^{(2)}$ and displacement $u_3^{(2)}$ of region (2) (indicated by the superscript) on the boundary $z=0$. The constant ν is Poisson's ratio and μ, λ Lamé constants with the subscripts indicating medium 1 and 2 respectively; γ's are functions of these elastic constants.

To solve this with a mixed boundary condition, a uniform circular indentation $u_3^{(2)}=\delta_0$ on $z=0$ for $r\le a$ and $\sigma_{33}^{(2)}=0$ for $r>a$ and , an integral representation is derived for $u_3^{(2)}$ on $z=0$. The approach taken is similar to that used in Atkinson and Chen (2005) (cf. Green and Zerna 1968) by modelling the problem with a continuous function $g(t)$. To achieve this, it is assumed that $\sigma_{33}^{(2)}=\frac{-it}{(r^2+(it)^2)^{3/2}}$ on the boundary $z=0$ with $r^2=x^2+y^2$ which has double Fourier transform $\bar{\bar{\sigma}}_{33}^{(2)}=-2\pi e^{-it(\xi^2+\zeta^2)^{1/2}}$, ξ and ζ being Fourier transform variables. Using the stress-displacement relation (A.1) the displacement $\bar{\bar{u}}_3^{(2)}$ (denoted by $\bar{\bar{u}}$ on $z=0$) can be written in terms of the stress $\bar{\bar{\sigma}}_{33}^{(2)}$ (denoted by $\bar{\bar{\sigma}}$ on $z=0$) as

$$\bar{\bar{u}} = 2\pi\left(\frac{1-\nu_2}{\mu_2}\right)\frac{e^{-it\rho}}{\rho} - 2\pi e^{-it\rho}\left[\frac{1}{\kappa(\rho,h)} + \left(\frac{1-\nu_2}{\mu_2}\right)\frac{1}{\rho}\right], \quad \rho = (\xi^2+\zeta^2)^{1/2}. \tag{A.2}$$

An integral expression for $u_3^{(2)}$ is derived by first inverting $\bar{\bar{u}}$ in the above equation, which is then multiplied by a continuous function $g(t)$ and integrated over t from 0 to a, then taking the real part to give

$$u_3^{(2)} = \left(\frac{1-\nu_2}{\mu_2}\right)\mathrm{Re}\left(\int_0^a \frac{g(t)\mathrm{d}t}{(r^2-t^2)^{1/2}}\right) - \mathrm{Re}\left(\int_0^a Q(t,r)g(t)\mathrm{d}t\right), \tag{A.3}$$

where

$$Q(t,r) = \int_0^{2\pi} \mathscr{F}(\rho,h)e^{-it\rho}J_0(-\rho r)\mathrm{d}\rho, \tag{A.4}$$

with J_0 being a Bessel function and

$$\mathscr{F}(\rho,h) = \frac{\rho}{\kappa(\rho,h)} + \left(\frac{1-\nu_2}{\mu_2}\right). \tag{A.5}$$

Assuming that the displacement $u_3^{(2)} = \delta_0$, a constant, within the contact region, the equation is inverted to give the integral equation for $g(u)$ as

$$g(u) = \frac{2}{\pi}\left(\frac{\mu_2}{1-\nu_2}\right)\delta_0 + \frac{2}{\pi}\left(\frac{\mu_2}{1-\nu_2}\right)\int_0^a g(t)I(u,t)\mathrm{d}t, \tag{A.6}$$

for $0 < u < a$, where

$$I(u,t) \quad = \quad \int_0^\infty \mathscr{F}(\rho,h)\cos(u\rho)\cos(t\rho)\mathrm{d}\rho. \tag{A.7}$$

The function $g(u)$ can be evaluated numerically for $0 < u < a$ when h, the thickness of the contact layer, is finite and subsequently the total force acting on the circular region is derived using equation (2.1)

When $h << a$, the numerical solution for $g(u)$ using the integral equation above diverges at the point $u = a$ and so a singular perturbation technique is employed to derive the solution for $g(u)$ near $u = a$ in the limit $h \to 0$ by defining an inner coordinate system,

$$u = a + \varepsilon X, \quad t = a + \varepsilon T, \quad \varepsilon\rho = \eta, \quad \text{for } -a/\varepsilon < X,\ T < 0, \tag{A.8}$$

and $h=\varepsilon$ with $G(X)=g(a+\varepsilon X)$. Thus equation (A.6) written in inner coordinates is now

$$G_-(X)=\frac{2\delta_0}{\pi}\left(\frac{\mu_2}{1-\nu_2}\right)+\frac{2}{\pi}\left(\frac{\mu_2}{1-\nu_2}\right)\int_{-a/\varepsilon}^{0}G_-(T)\,I(X,T)\,\mathrm{d}T\,, \tag{A.9}$$

for $-a/\varepsilon<X<0$. The definition for $G(X)$ is extended so that for $X>0$,

$$G_+(X)=\frac{2}{\pi}\left(\frac{\mu_2}{1-\nu_2}\right)\int_{-\infty}^{0}G_-(T)\,I(X,T)\,\mathrm{d}T. \tag{A.10}$$

Taking the Fourier Transform of $G_+(X)$ and $G_-(X)$ with

$$\overline{G}_-(\xi)=\int_{-\infty}^{0}G_-(X)\,e^{i\xi X}\,\mathrm{d}X \quad \text{and} \quad \overline{G}_+(\xi)=\int_{0}^{\infty}G_+(X)\,e^{i\xi X}\,\mathrm{d}X, \tag{A.11}$$

where the subscripts '+' and '-' of the half Fourier transform $G_-(\xi)$ and $G_+(\xi)$ denote regions of upper and lower half-planes of regularity and ignoring the higher order terms gives

$$\frac{\overline{G}_-(\xi)}{q(|\xi|)}-\frac{2}{\pi}\left(\frac{\mu_2}{1-\nu_2}\right)\frac{\delta_0}{i\xi}=-\overline{G}_+(\xi), \tag{A.12}$$

and

$$q(|\xi|)=\frac{\gamma_5+\gamma_3\,|\xi|^2\,e^{-2|\xi|}+\gamma_1\,e^{-2|\xi|}+\gamma_4\,e^{-4|\xi|}}{\gamma_5-\gamma_3\,|\xi|\,e^{-2|\xi|}-\gamma_4\,e^{-4|\xi|}}, \tag{A.13}$$

where $\gamma's$ being functions of the elastic constants are given by

$$\begin{aligned}
\gamma_1 &= \frac{\gamma_2}{\mu_2^2(3\mu_1+\lambda_1)(\lambda_2+3\mu_2)(\lambda_2+\mu_2)},\\
\gamma_2 &= \mu_2^2(\lambda_2+\mu_2)(2\mu_1^2+(\lambda_2+\mu_2)(\lambda_1+3\mu_1))-\mu_1^2(\lambda_1+\mu_1)(4\mu_2(\lambda_2+\mu_2)\\
&\quad +(\lambda_2^2+\mu_2^2)),\\
\gamma_3 &= \frac{16(\lambda_2+\mu_2)(\lambda_1\mu_2+3\mu_1\mu_2+\lambda_1\mu_1+\mu_1^2)(\mu_2-\mu_1)}{\mu_2^2(3\mu_1+\lambda_1)(\lambda_2+3\mu_2)},\\
\gamma_4 &= \frac{4(\mu_1-\mu_2)((\lambda_1-\mu_1)(\lambda_2\mu_1-3\mu_1\mu_2)-(\lambda_2-\mu_2)(\lambda_1\mu_2-3\mu_1\mu_2))}{\mu_2^2(3\mu_1+\lambda_1)(\lambda_2+3\mu_2)},\\
\gamma_5 &= \frac{4(\lambda_1\mu_2+3\mu_1\mu_2+\lambda_1\mu_1+\mu_1^2)((\mu_2^2+\lambda_2\mu_2+3\mu_1\mu_2+\lambda_2\mu_1)}{\mu_2^2(3\mu_1+\lambda_1)(\lambda_2+3\mu_2)}.
\end{aligned}$$

Equation (A.12) is rewritten to give the Wiener-Hopf equation

$$\frac{\overline{G}_-(\xi)}{q_-(\xi)} - \frac{2}{\pi}\left(\frac{\mu_2}{1-\nu_2}\right)\frac{\delta_0}{i\xi}\,q_+(0) = \\ -\overline{G}_+(\xi)\,q_+(\xi) + \frac{2}{\pi}\left(\frac{\mu_2}{1-\nu_2}\right)\frac{\delta_0}{i\xi}\,(q_+(\xi)-q_+(0)) = L(\xi), \quad \text{(A.14)}$$

where

$$q_-(\xi) = q_-(0)\left(1 - \frac{m_0}{\pi}\,(i\xi) - \frac{m_1}{\pi}\,(i\xi)\log(i\xi) - m_2\,(i\xi)^2\log(i\xi) + \cdots\right), \\ \text{as} \quad \xi \to 0, \quad \text{(A.15)}$$

and

$$m_0 = -\int_0^\infty \log y\,\frac{\mathrm{d}}{\mathrm{d}y}\left(\frac{f(y)}{y}\,\mathrm{d}y\right), \quad f(y) = \tan^{-1}\left(\frac{\mathrm{Im}\,q(-iy)}{\mathrm{Re}\,q(-iy)}\right), \quad \text{(A.16)}$$

with $q_-(0) = q_+(0) = q_0^{1/2}$ and

$$q_0 = \frac{\mu_1(1-\nu_2)}{\mu_2(1-\nu_1)}, \quad m_1 = 2\left(\frac{\gamma_5-\gamma_4}{\gamma_1+\gamma_4+\gamma_5}\right) - \frac{2(\gamma_4+\gamma_5)-\gamma_3}{\gamma_5-\gamma_4}. \quad \text{(A.17)}$$

Note that m_2 does not appear in the expansion for $G_-(X)$ below or the subsequent expansion for the total force. Using analytic continuation, the function $L(\xi)$ is thus analytic in the whole ξ-plane and both sides of the equation are bounded for large ξ. Applying Liouville's theorem with $L(\xi) = A/i\xi$, an expansion for $G_-(\xi)$ in the limit $\xi \to \infty$ can be obtained and inverted to give $G_-(X)$ as $X \to 0$. The constant A, which we expect to be of order ε, is unknown as a consequence of resacling with inner coordinates and is obtained through matching with the outer solution. Here we follow the matching principle of Van Dyke and matching a two-term inner solution written in three-term outer with a three-term outer solution written in two-term inner. The three-term outer solution is

$$g^{(o)}(u) = \frac{2\,\delta_0}{\pi}\left(\frac{\mu_1}{1-\nu_1}\right) \\ + h\left\{\beta_0\left(\frac{1}{a-u}+\frac{1}{a+u}\right) + \alpha_0\left[1 + C_1\left(\frac{\mu_2}{1-\nu_2}\right)\right]\delta(a-u)\right\} \\ + h^2\left\{\gamma_0\left[\log(a-u)+\log(a+u)\right] - \alpha_0\,\frac{C_2}{\pi}\left(\frac{\mu_2}{1-\nu_2}\right)\left(\frac{1}{(a-u)^2}+\frac{1}{(a+u)^2}\right)\right\}, \quad \text{(A.18)}$$

with α_0, β_0 and γ_0 being unknown. Matching gives

$$A = \frac{h\,\delta_0}{a\,\pi}\left[\frac{\mu_1\,\mu_2}{(1-\nu_1)(1-\nu_2)}\right]^{1/2}\frac{m_1}{\pi}, \tag{A.19}$$

and so inverting $G_-(\xi)$ above, taking the limit $\xi \to \infty$, $q_-(\xi) \to 1$, we obtain

$$G_-(X) = \frac{2\,\delta_0}{\pi}\left[\frac{\mu_1\,\mu_2}{(1-\nu_1)(1-\nu_2)}\right]^{1/2}\left(1+\frac{h}{2a}\frac{m_1}{\pi}\right), \quad X \to 0-. \tag{A.20}$$